



## Bis(dibenzoylmethanato)Zirconium(IV) Chloride Complex as a Potential Catalyst for the Ring Opening Polymerization of $\delta$ -Valerolactone

Muhammad Yusuf; Eddiyanto Eddiyanto; Rudi Munzirwan Siregar; Rizki Dwi Irmalasari

*<sup>a</sup>Department of Chemistry, Universitas Negeri Medan, Jl. Willem Iskandar, Medan, 20221, Indonesia*



CrossMark

### Abstract

Poly( $\delta$ -valerolactone) (PVL) and its copolymers are currently widely used in medical applications such as drug delivery systems, implants, tissue engineering, and packaging. In the medical field, PVL is one of the most commonly used materials because it is biocompatible, flexible, and non-toxic. To produce PVL, ring opening polymerization (ROP)  $\delta$ -valerolactone ( $\delta$ -VL) will be performed using a complex catalyst bis(dibenzoylmethanato)zirconium(IV) chloride ( $\text{bis(dibzm)}_2\text{Zr}$ ). The advantage of this catalyst is that it can be utilized in the tropics because it is not sensitive to water vapor and air. Moreover, the Lewis acidity of the central atom can also be controlled by varying the electron-withdrawing and electron-donating groups of the ligands. The PVL product characterization in this research was carried out by using FTIR,  $^1\text{H}$ NMR,  $^{13}\text{C}$ NMR, XRD, DSC, and TGA. The obtained PVL is semicrystalline with a low melting point. Thus, the obtained PVL can be applied as a medical material and biodegradable packaging.

**Keywords:** Ring opening polymerization,  $\delta$ -valerolactone, bis(dibenzoylmethanato)-zirconium(IV) chloride, Poly( $\delta$ -valerolactone)

### Introduction

In the twenty-first century, green materials such as polylactones are becoming more popular in the medical field for use in artificial implants, tissue engineering, drug delivery, and wound dressings. Polylactones have biocompatibility, non-toxic, and thermoplastic properties, so that they are widely used as medical materials, including implant materials. After use, implants are easily removed from the body in the form of small molecules that decompose quickly and do not cause poisoning [1–3]. Apart from in the medical field, polylactones are also used as biodegradable packaging because polylactones contain a carbonyl group [4]. Furthermore, the microbe will come into contact with the polylactone, causing it to change its nature and become more hydrophilic. As a result, the polymer surface has the potential ability to absorb water, thus making the degradation process by bacteria easier [5].

Over the last few years, poly( $\delta$ -valerolactone) (PVL) which is part of polylactones has become the main choice for use as medical

materials, especially in drug delivery systems. So far, PVL has been used as a drug delivery agent to the skin for antifungal drugs. Additionally, PVL has also been used as a delivery system for chemotherapy drugs such as the anthracycline antibiotic daunorubicin (DNR) and several other hydrophobic drugs. DNR is an antitumor drug used in the treatment of lung, bladder, breast, ovarian, lymphoma, brain, and lymphocytic leukemia [6]. The use of PVL as one of the most desirable materials in the medical field is due to its ease of processing, low melting point, non-toxic, semi-crystalline, and flexibility. Until now, various efforts by various researchers to improve the quality of PVL as a medical material have continued to be carried out by means of synthesis, blending, and copolymers.

PVL (poly( $\delta$ -valerolactone)) is a type of polymer obtained through ROP. ROP is the preferred reaction route in ring opening because of its ease of carrying out polymerization reactions based on its thermodynamic and kinetic factors. ROP is a chain growth reaction in which the reactive center is located at the terminal end of the polymer [7]. This reactive center will react with other monomers

\*Corresponding author e-mail: [myusuf@unimed.ac.id](mailto:myusuf@unimed.ac.id); (Muhammad Yusuf).

Receive Date: 26 November 2021, Revise Date: 15 March 2022, Accept Date: 24 March 2022

DOI: 10.21608/EJCHEM.2022.107965.4942

©2022 National Information and Documentation Center (NIDOC)

resulting in ring opening, propagation, and polymer chain elongation. Some of the catalysts used in ROP  $\delta$ -VL include hydrochloric acid [1], tris(pentafluorophenyl)borane [5], boric acid [6], Triazabicyclo-[4.4.0]dec-5-ene (TBD) [10], 2,6-Bis(amino)phenol Zinc Complex [11], copper diketiminate complexes [12], Benzoheterocyclic Ureas/MTBD [13], distannoxane [14], [15], and Yttrium [16]. However, some of these catalysts have a weakness because it is necessary to add an initiator and a cocatalyst that is sensitive to air. As a result, extra handling is required when performing the ROP of  $\delta$ -VL.

Unlike the previous catalyst, the bis(dibzm)Zr catalyst complex does not require the addition of an initiator and cocatalyst during ROP  $\delta$ -VL. Moreover, this catalyst is easier to handle when reacted, so that it is suitable for being used as a catalyst in  $\delta$ -VL ROP. We previously reported on the use of a bis(dibzm)<sub>2</sub>Zr catalyst complex in the ROP of  $\varepsilon$ -CL to produce PCL [17]. In this paper, we will describe a simple ROP  $\delta$ -VL method based on a bis(dibzm)<sub>2</sub>Zr catalyst complex. In addition, we also characterized the physical and chemical properties of the resulting PVL by using FTIR, <sup>1</sup>HNMR, <sup>13</sup>CNMR, XRD, DSC, and TGA.

## Experimental

### Material and Methods

The Sigma-Aldrich company provided the chemicals used in this study, including the  $\delta$ -VL, dibenzoylmethane ligand, and ZrCl<sub>4</sub>. DSC and XRD characterization were used to determine the physical properties of PVL. Meanwhile, FTIR, <sup>1</sup>HNMR, and <sup>13</sup>CNMR were used to determine the chemical characteristics of PVL.

The FTIR spectroscopy was measured using a Perkin-Elmer spectrometer while the shape of the sample used was in the form of solid KBr pellets. Next, the measurements of <sup>1</sup>H NMR and <sup>13</sup>C NMR were analysed using an Agilent 500 spectrometer at 500 MHz in CDCl<sub>3</sub> solvent. Then, Shimadzu XRD-6100 diffractometer was used to measure X-ray powder diffractions (XRD) with Cu-K $\alpha$  radiation. Meanwhile, the measurements of DSC were analysed by using the SHIMADZU DSC-60 Plus Series at a scanning speed of 10 °C/min, which covers a temperature range between 27 °C and 500 °C. Last, DTG 60 Shimadzu was used to perform thermogravimetry analysis of PVL at 10 °C/min with a heating range from 36 °C to 600 °C in a nitrogen atmosphere [17].

### Synthesis of Bis(dibenzoylmethanato)-Zirconium(IV) Chloride

A total of 0.93 g of zirconium tetrachloride (4 mmol) was mixed with 2.16 g of dibenzoylmethanato ligand (9.6 mmol) and refluxed using 20 mL of benzene as solvent. The reaction was carried out for 14 hours at a temperature of 85 °C. Next, the cooling process is carried out until a solid product is formed while the filtrate is removed. After that, the complex formed was washed three times using n-hexane with a volume of 8 mL. The final step is drying the bis(dibzm)<sub>2</sub>Zr complex catalyst using vacuum [18]. [Zr(dibzm)<sub>2</sub>]Cl<sub>2</sub>: Yield 59%.

### Ring-Opening Polymerization of $\delta$ -Valerolactone

ROP  $\delta$ -VL was carried out in the following manner: At 100 °C for 4 hours,  $\delta$ -VL monomer (3.9 g, 38 mmol) and bis(dibzm)<sub>2</sub>Zr (0.12 g, 0.19 mmol) were reacted. After that, the product was cooled at room temperature and dissolved in 15 mL of chloroform and also stirred for 3 hours. To yield a clear solution, the PVL was refluxed for 1 hour. Next, PVL was precipitated with 20 mL of diethyl ether and then vacuumed to obtain dry PVL. Last, FTIR, XRD, DSC, <sup>1</sup>HNMR, and <sup>13</sup>CNMR instruments were used to characterize the PVL products. Yield 82% [14].

## Results and Discussion

The primary goal of this investigation is to use the bis(dibzm)<sub>2</sub>Zr complex as a catalyst in the ROP  $\delta$ -VL. The resulting PVL was analyzed using FTIR, <sup>1</sup>HNMR, <sup>13</sup>CNMR, XRD, DSC, and TGA.

### Characterization of Bis(dibenzoyl-methanato) Zirconium(IV) Chloride Complex Compound

In this investigation, the complex was characterized using XRD and <sup>1</sup>HNMR.

#### XRD Analysis of complex catalyst

The XRD diffractogram pattern of the [bis(dibzm)<sub>2</sub>]Zr]Cl<sub>2</sub> complex catalyst is shown in Figure 1. The diffractogram pattern of the complex was different from the patterns of the two reactants of it, the dibzm ligand and ZrCl<sub>4</sub>. Whereas, the XRD pattern of ZrCl<sub>4</sub> can be seen from the results obtained by Liu's research group [19]. These results indicate that the catalyst complex [bis(dibzm)<sub>2</sub>]Zr]Cl<sub>2</sub> has been formed.

#### <sup>1</sup>HNMR Analysis of complex catalyst

An NMR analysis was carried out to determine the structure of the [bis(dibzm)<sub>2</sub> Zr]Cl<sub>2</sub> complex catalyst by observing the chemical shifts of atoms in different electronic environments.

Figure 2 shows a typical <sup>1</sup>H-NMR spectrum of complex.

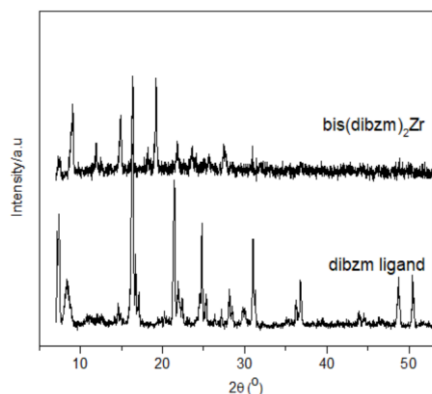


Figure 1: XRD analysis of bis(dibzm)<sub>2</sub>Zr complex

In addition, Table 1 also displays the detailed data for proton resonance of [bis(dibzm)<sub>2</sub>Zr]Cl<sub>2</sub> complexes. The <sup>1</sup>H NMR complex signal (500 MHz, CDCl<sub>3</sub>) that appears at 7.213 ppm is a proton of Ha (s, 1H). Next, the signal that appears at 7.375 -7.456 ppm is a proton of Hb (t, 4H). Then, the signal that appears at 1.7 ppm is a proton of Hc 7.479-7.543 (t, 2H). Last, the signal that appears at 8.065-8.202 ppm is proton of Hd (d, 4H). The results of the <sup>1</sup>H NMR analysis of the complex compound were identical to those found by other researchers [18].

Table 1. <sup>1</sup>H resonances of bis(dibzm)<sub>2</sub>Zr

H position	Chemical shift/ ppm	Integrated intensity	
		calculated	observed
a	7.213 (s)	1	1
b	7.375 -7.456 (t)	4	4
c	7.479-7.543 (t)	2	3
d	8.065-8.202 (d)	4	4

s = singlet; t = triplet; d = duplet

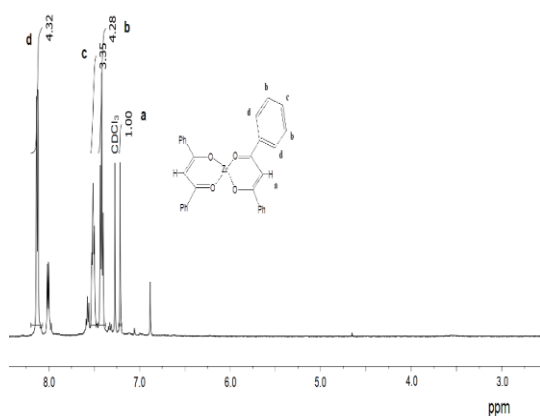


Figure 2: <sup>1</sup>H NMR spectrum of bis(dibzm)<sub>2</sub>Zr complex

## Ring-Opening Polymerization of $\delta$ -Valerolactone

In this investigation, the resulting PVL was characterized using FTIR, NMR, XRD, DSC and TGA.

### FTIR Analysis of PVL

The PVL spectra obtained using a bis(dibzm)<sub>2</sub>Zr catalyst are shown in Figure 3.

The FTIR spectra of PVL showed that the CH<sub>2</sub> asymmetric at 2949 cm<sup>-1</sup>, CH<sub>2</sub> symmetric at 2877 cm<sup>-1</sup>, carbonyl (C=O) at 1721 cm<sup>-1</sup>, CH asymmetric elongation at 1457 cm<sup>-1</sup>, CH<sub>2</sub> bending at 1319 cm<sup>-1</sup>, C-C at 1257 cm<sup>-1</sup>, C-O at 1165 cm<sup>-1</sup>, and long chain methylene rock at 740 cm<sup>-1</sup>. The results obtained have the same infrared band as those obtained by other researchers [9].

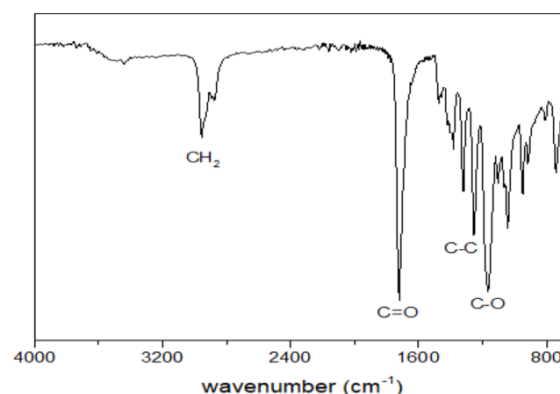


Figure 3: The FTIR spectrum of PVL generated by bis(dibzm)<sub>2</sub>Zr catalyst

### NMR Analysis of PVL

An NMR analysis was performed to determine the structure of the resulting PVL by observing the chemical shifts of atoms in different electronic environments.

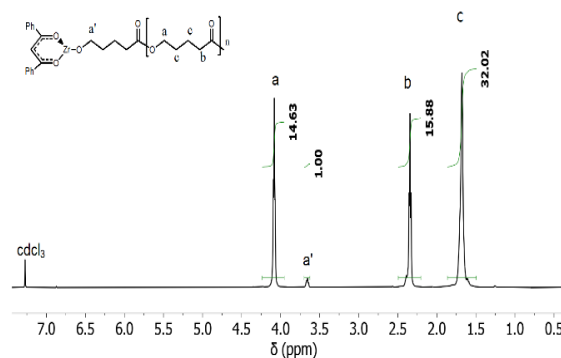


Figure 4: <sup>1</sup>H-NMR spectrum of PVL

Figure 4 shows a typical  $^1\text{H-NMR}$  spectrum of PVL. The  $^1\text{HNMR}$  PVL signal (500 MHz,  $\text{CDCl}_3$ ) that appears at 4.1 ppm is a proton of methylene bound to an ester bond (Ha). Meanwhile, the signal that appears at 2.4 ppm is a methylene proton bound to a carbonyl group (Hb). The signal that appears at 1.7 ppm is a methylene proton at the center of the PVL structure (Hc). Finally, the signal that appears at 3.6 ppm is the methylene proton at the end of the PVL chain (Ha'). The results of the  $^1\text{HNMR}$  PVL analysis obtained are alike to those obtained by previous researchers [10] [20].

On the other hand, PVL polymer degree (DP) analysis was also carried out by using the  $^1\text{HNMR}$  integration comparison method. The method is to compare the ratio of repeated units integration (Ha, Hb, Hc) to the integration of methylene at the end of the polymer chain (Ha') [21]. Some of the  $^1\text{H}$  NMR PVL data required for DP determination are shown in Table 2.

Table 2. Determination the degree of PVL polymerization by using  $^1\text{H-NMR}$  data

Feature	Moiety	$\delta$ (ppm)	Peak area
End group (Ha')	$\text{CH}_2$	3.6	1
Repeating units (Ha,Hb,Hc)	$\text{C}_4\text{H}_8$	4.1; 2.4; 1.7	62

To calculate DP PVL (n), we need data on the peak area of the end group ( $a\text{CH}_2 = 1$ ), the peak area of repeating units ( $a\text{C}_4\text{H}_8=62$ ), the number of H atoms in the end group ( $m\text{CH}_2 = 2$ ), the number of H atoms in repeating units ( $m\text{C}_4\text{H}_8= 8$ ), and the number of repeating units of the end group ( $n\text{CH}_2 = 1$ ). This data is then substituted into equation 1 [22].

$$\begin{aligned} n\text{PVL} &= \frac{a\text{C}_4\text{H}_8 \cdot m\text{CH}_2 \cdot n\text{CH}_2}{a\text{CH}_2 \cdot m\text{C}_4\text{H}_8} \quad \text{eq.1} \\ &= \frac{62 \times 2 \times 1}{1 \times 8} \\ &= 15,5 = 15 \end{aligned}$$

The DP PVL obtained in this study was 15, based on the calculation results (eq.1). The low DP obtained can be caused by various factors. These factors include deactivation of the catalyst, steric hindrance from complex compounds, and the length of the PVL chain. As a result, it is difficult for  $\delta\text{-VL}$  to perform insertions as illustrated in Scheme 1. The low temperature factor can also be the cause of the low DP because it can cause a slowdown in translational motion, vibration, and rotation of the molecule.

Previously, several other researchers have also explored research on  $\delta\text{-VL}$  polymerization using

a catalyst. As a result, they obtained PVL with a higher DP as described in Table 3.

Table 3. DP PVL was obtained using several catalysts.

Catalyst	t(h)	T ( $^\circ\text{C}$ )	DP
$\text{ZrCl}_4$	4	100	0
$\text{Bis(dibzm)}_2\text{Zr}$	4	100	15
Boric acid [6]	70	130	44
$\text{B}(\text{C}_6\text{F}_5)_3$ [5]	4	80	96
Benzoheterocyclic	0.14	25	96
Ureas/MTBD [13]			
Bis(amino)Ph Zinc [11]	0.14	30	247

The high DP of PVL (44 to 247) obtained by other researchers was due to the catalyst having a higher activity compared to  $\text{Bis(dibzm)}_2\text{Zr}$  complex catalyst. As a result, the catalyst can still be inserted into the PVL even though the chain is getting longer. As a result, a PVL with a higher DP was obtained. On the other hand, if the  $\delta\text{-VL}$  polymerization reaction is carried out using  $\text{ZrCl}_4$  substrate as a catalyst, there is no polymerization reaction occurs. Besides that, other researchers also added the initiator of benzyl alcohol (BnOH) during the reaction so that the initiation process of the polymerization reaction could take place more easily. Meanwhile, PVL has good solubility in chloroform, acetone, and THF [1].

The results of the  $^{13}\text{C-NMR}$  analysis are shown in Figure 5. The PVL signals obtained from the  $^{13}\text{C-NMR}$  spectrum are: 175, 65, 32, 28, 20, and 61. The signal is the carbon of the carbonyl appearing at 175 ppm (a). Furthermore, carbon from methylene at the center of the PVL structure appeared at 32 ppm (b), 28 ppm (d), and 20 ppm (c). While the carbon attached to the ester group appears at 65 ppm (e). The carbon at the end of the PVL chain appears at 61 ppm (e'). The results of the  $^{13}\text{CNMR}$  PVL analysis obtained are alike to those obtained by previous researchers. The  $^{13}\text{CNMR}$  analysis also indicated that the PVL obtained had a linear structure due to the absence of a signal appearing at around 40 ppm [15].

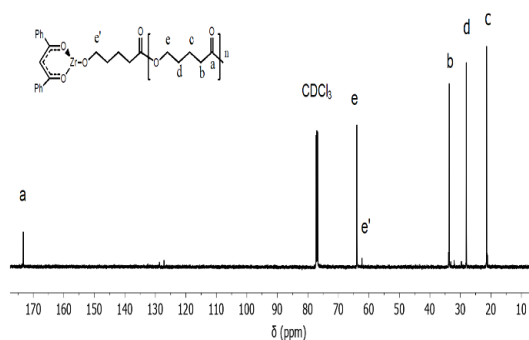
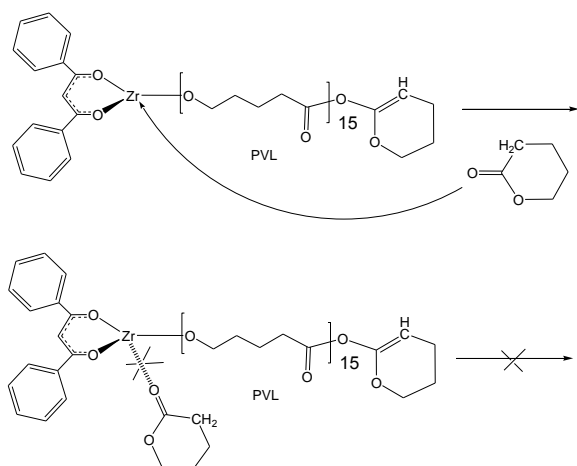


Figure 5:  $^{13}\text{C-NMR}$  spectrum of PVL



Scheme 1: The proposed mechanism for the difficulty of  $\delta$ -VL insertion in PVL

### XRD (X-Ray Diffraction) Analysis of PVL

XRD analysis was performed to observe the crystalline and amorphous structure of the resulting PVL. The crystalline peak will be sharp, whereas the amorphous peak will be broad [23].

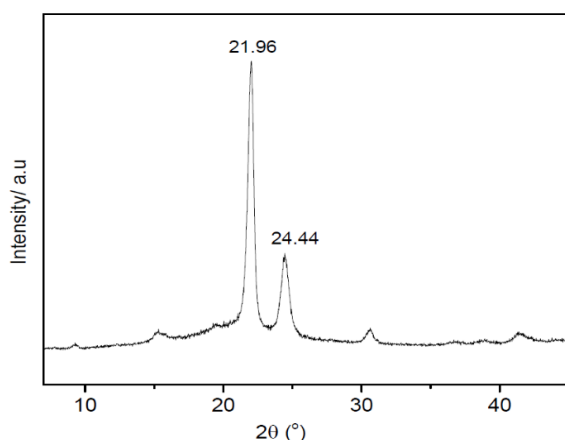


Figure 6: XRD analysis of PVL

Based on Figure 6, PVL was observed to have crystalline and amorphous peaks. The PVL crystalline phase in the XRD results was indicated by the presence of two sharp peaks at an angle of  $21.96^\circ$  and  $24.44^\circ$ . These peaks are identified according to the lattice planes (110) and (200). Therefore, the crystal structure of PVL is orthorhombic, where the crystallite size of D110 is 16.21 nm. Meanwhile, the crystallite size of the D200 is approximately 12.56 nm (Table 4) [1] [8].

The degree of crystallinity ( $X_c$ ) of PVL obtained in this study was 62%. The  $X_c$  calculation method have identical method to those used in earlier

investigations [9]. The crystalline phase of PVL has a more regular structure. In this section, the structure will be more rigid because of the strong bonds between atoms in the PVL structure. Unlike the PVL crystalline phase, the amorphous phase appears to be widened whose  $2\theta$  angle is other than the crystalline phase. While the amorphous part of PVL has an irregular structure with a percentage of 38%. Thus, these results indicate that PVL is a semicrystalline polymer with a flexible structure, so that it is suitable for use for medical purposes [10].

On the other hand, PVL is also easily biodegradable because it has an amorphous phase. This phase will be more easily degraded than the crystalline phase because it has a less regular structure [15]. After that, the amorphous phase will be added as a result of the biodegradation process using microbes, and there will be a decrease in the crystallinity of PVL.

Table 4. Crystallite Size (nm) for PVL (110), and (200) Orientation Planes

Crystallite size	$2\theta$	nm	$X_c$ (%)
D110	21.97	16.21	62
D200	24.45	12.56	

### DSC Analysis of PVL

DSC analysis was performed to provide information on the glass transition temperature ( $T_g$ ), crystallization ( $T_c$ ), and melting point ( $T_m$ ). The glass transition state ( $T_g$ ) is the phase in which the polymer changes to a rubber-like material (rubbery) from the solid state. Crystallization point ( $T_c$ ) is the temperature at which the polymer is crystalline. The melting point ( $T_m$ ) is the temperature at which the polymer is a liquid. While in this study, DSC was used to measure the melting point of PVL.

The PVL obtained in this study has a  $T_m$  value of  $56.41^\circ\text{C}$  with an enthalpy ( $\Delta H_m$ ) of 106.53 J/g as shown in Figure 7. The resulting PVL melting point curve is also relatively sharp. Both the  $T_m$  value and the  $T_m$  curve obtained are alike to be the results obtained by previous researchers [20], [24]. On the other hand, the low value ( $T_m$ ) of PVL is caused by its natural characteristics, such as structure, bonding, and molecular weight. Meanwhile, the low melting point of PVL makes it easy to combine with other materials for use as medical materials and biodegradable packaging.

In the other hand, the  $T_g$  temperature of PVL is in the range of  $-60^\circ\text{C}$ . In this study,  $T_g$  could not be measured because the lowest temperature limit of the DSC instrument used was only  $27^\circ\text{C}$  [1], [25].

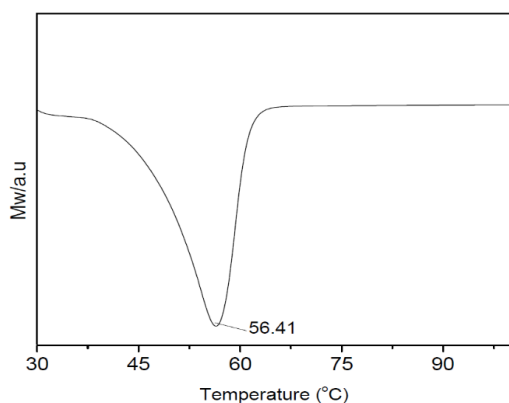


Figure 7: DSC analysis of PVL

### TGA Analysis of PVL

TGA analysis was conducted to provide information on the decomposition temperature ( $T_d$ ) of PVL.

In the Figure 8 shows the decomposition of PVL starting at a temperature of around 0 °C. In the temperature range of 0 °C to 115 °C, PVL decomposition occurs, resulting in a weight loss of 10%. In the temperature range of 115 °C to 284 °C, there was a dramatic decomposition of PVL, resulting in a weight loss of 95.8%. Finally, in the temperature range of 284 °C to 600 °C, PVL decomposition occurs until its weight becomes zero. The results obtained are alike to those obtained by the Jitonnom research group [24]. However, the decomposition temperature obtained was lower because the resulting polymer had a low DP (DP = 15). While the DP obtained by the Jitonnom research group was 187 [24].

The thermal degradation of PVL is explained via the unzip mechanism. In the early steps, PVL will be degraded into  $\delta$ -VL. After that, PVL will be degraded into 4-pentanoic acid and  $\text{CO}_2$ . Finally,  $\text{CO}_2$ ,  $\text{H}_2\text{O}$ , and methyl butanoate will be formed [26].

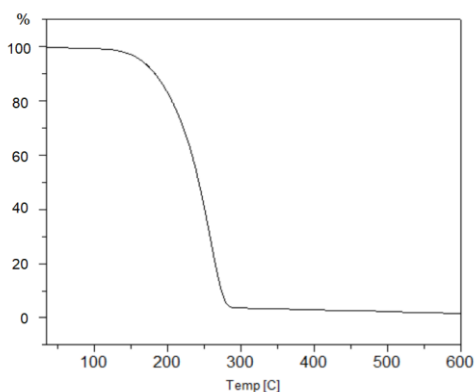
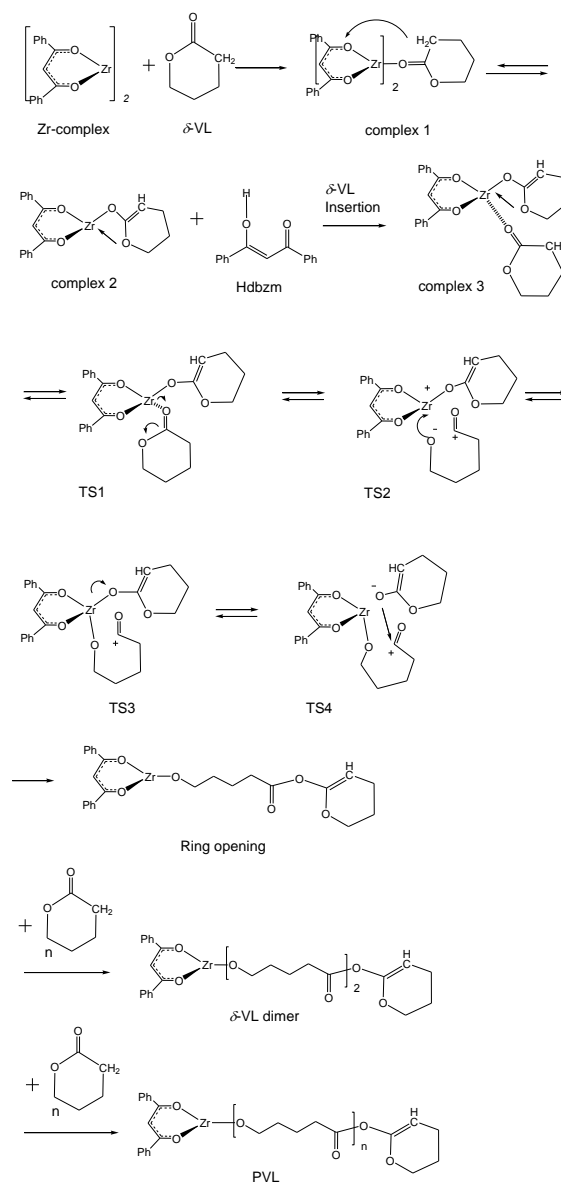


Figure 8: TGA analysis of PVL

### Reaction Mechanism

Scheme 2: The possible ROP of  $\delta$ -VL reaction mechanism pathway using a bis(dibzm) $_2$ Zr catalyst

The possible ROP of  $\delta$ -VL reaction mechanism starting from complex Zr to complex 3 has the same route as we reported in our earlier investigation [27], [28]. In this study, we will focus on the reaction mechanism from TS1 to TS4 as shown in Scheme 2. At TS1, the Zr-O coordination is released to form a positive charge on the  $\delta$ -VL carbonyl and a negative charge on the O atom. Then at TS2, the negatively charged O atom attacks the Zr atom so that a new Zr-O bond is formed. Then at TS3, the Zr-O bond will be released, resulting in a negative charge on the O atom. After that at TS4, the positively charged carbonyl C atom will be attacked

by the negatively charged O atom, causing the  $\delta$ -VL ring to open. The next step is the insertion of  $\delta$ -VL to form an  $\delta$ -VL dimer [29].

Some of the optimized molecular geometries are shown in Figure 9 including the bis(dibzm)<sub>2</sub>Zr complex,  $\delta$ -VL, and  $\delta$ -VL dimer.

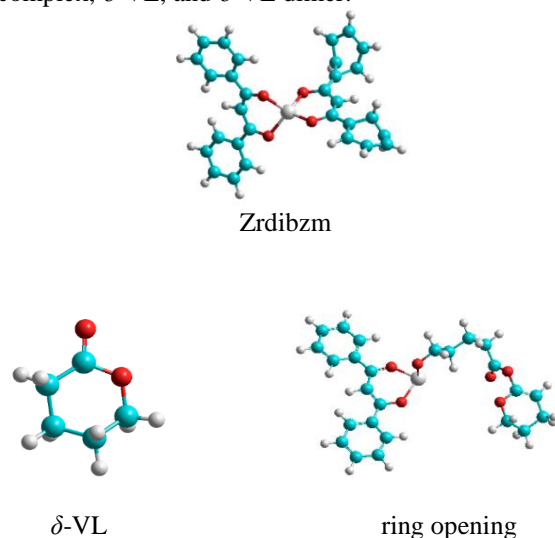


Figure 9: The molecular geometry of bis(dibzm)<sub>2</sub>Zr,  $\delta$ -VL, and  $\delta$ -VL dimer compounds

## Conclusion

The ROP of  $\delta$ -VL has been completed successfully using a bis(dibzm)<sub>2</sub>Zr complex catalyst at 100 °C for 4 hours. This catalyst is suitable for use in equatorial regions such as Indonesia because it is not sensitive to water vapor and air. Because of the Lewis acidity of the bis(dibzm)<sub>2</sub>Zr complex catalyst,  $\delta$ -VL can be easily inserted into the complex. Moreover, the  $\delta$ -VL insertion will be able to continue if the Lewis acid charge of the catalyst remains active.

On the other hand, the PVL obtained in this study has a semicrystalline structure, a low melting point, and a linear structure with a DP of 15 based on the results of FTIR, <sup>1</sup>HNMR, <sup>13</sup>CNMR, XRD, DSC, and TGA analysis. These properties are suitable for biomedical purposes that require biocompatibility, flexibility, non-toxicity, and biodegradable properties.

However, the low DP PVL (15) obtained indicates that there has been a faster deactivation of the catalyst so that the  $\delta$ -VL is difficult to insert. To get a higher DP PVL, further research needs to be done with variations in the use of Lewis acid catalysts, ligand variations, addition of cocatalysts, addition of initiators and increasing temperature.

## Conflicts of interest

There are no potential conflicts of interest.

## Acknowledgement

The author is grateful to Universitas Negeri Medan for its financial assistance and research facilities (PNBP No.123/UN 33.8/KEP/PPKM/2021).

## References

- [1] W. S. Saeed, A. B. Al-Odayni, A. Alrahlah, A. A. Alghamdi, and T. Aouak, "Preparation and characterization of poly( $\delta$ -Valerolactone)/TiO<sub>2</sub> nanohybrid material with pores interconnected for potential use in Tissue Engineering," *Materials (Basel)*, vol. 12, no. 3, 2019, doi: 10.3390/ma12030528.
- [2] A. A. Haroun, A. H. M. Osman, S. A. Ahmed, and A. H. Elghandour, "Beta-cyclodextrin grafted with poly ( $\epsilon$ -caprolactone) for ibuprofen delivery system," *Egypt. J. Chem.*, vol. 62, no. 5, pp. 1227–1235, 2019, doi: 10.21608/EJCHEM.2018.5125.1455.
- [3] H. Elsayed and S. Ibrahim, "Biodegradable package films of poly(L-Lactic) acid/extracted gelatin blend from white leather fibers," *Egypt. J. Chem.*, vol. 63, no. 8, pp. 3059–3074, 2020, doi: 10.21608/EJCHEM.2020.23131.2369.
- [4] I. M. Arcana, M. Hasan, S. D. Anggraini, A. A. Febrianti, and A. Ardana, "Structure and Properties of Polymers Prepared by Polymerization of 2,2-Dimethyl-1,3-Propandiol and  $\epsilon$ -Caprolactone Monomer," *ITB J. Sci.*, vol. 41, no. 2, pp. 78–87, 2009, doi: http://dx.doi.org/10.5614%2Fitbj.sci.2009.41.2.2.
- [5] J. Xu, J. Song, S. Pispas, and G. Zhang, "Metal-free controlled ring-opening polymerization of  $\epsilon$ -caprolactone in bulk using tris(pentafluorophenyl)borane as a catalyst," *Polym. Chem.*, vol. 5, no. 16, pp. 4726–4733, 2014, doi: 10.1039/c4py00342j.
- [6] K. Duale, M. Zi, P. Chaber, D. Jeanne, and D. Fouque, "Molecular Level Structure of Biodegradable Poly ( Delta-Valerolactone ) Obtained in the Presence of Boric Acid," *Molecules*, vol. 23, no. 8, p. 2034, 2018, doi: 10.3390/molecules23082034.
- [7] G. Cama, D. E. Mogosanu, A. Houben, and P. Dubruel, *Synthetic biodegradable medical polyesters: Poly- $\sigma$ -caprolactone*. Elsevier Ltd, 2017.
- [8] M. Badwelan *et al.*, "Poly( $\delta$ -valerolactone)/poly(ethylene-co-vinylalcohol)/  $\beta$ -tricalcium phosphate composite as scaffolds: Preparation, properties, and in vitro amoxicillin

- release,” *Polymers (Basel)*, vol. 13, no. 1, pp. 1–22, 2021, doi: 10.3390/polym13010046.
- [9] W. S. Saeed, A. B. Al-Odayni, A. A. Alghamdi, A. Alrahlah, and T. Aouak, “Thermal properties and non-isothermal crystallization kinetics of poly ( $\delta$ -valerolactone) and poly ( $\delta$ -valerolactone)/titanium dioxide nanocomposites,” *Crystals*, vol. 8, no. 12, pp. 1–24, 2018, doi: 10.3390/cryst8120452.
- [10] Y. Ren *et al.*, “Synthesis of highly branched poly( $\delta$ -valerolactone)s: A comparative study between comb and linear analogues,” *RSC Adv.*, vol. 6, no. 51, pp. 45791–45801, 2016, doi: 10.1039/c6ra09289f.
- [11] Q. Hu, S. Jie, P. Braunstein, and B. Li, “Ring-opening Copolymerization of  $\epsilon$ -Caprolactone and  $\delta$ -Valerolactone Catalyzed by a 2, 6-Bis ( amino ) phenol Zinc Complex,” *Chinese J. Polym. Sci.*, vol. 38, pp. 240–247, 2019, doi: 10.1007/s10118-020-2347-4.
- [12] T. J. J. Whitehorne and F. Schaper, “Lactide,  $\beta$ -butyrolactone,  $\delta$ -valerolactone, and  $\epsilon$ -caprolactone polymerization with copper diketiminate complexes,” *Can. J. Chem.*, vol. 92, no. 3, pp. 206–214, 2014, doi: 10.1139/cjc-2013-0392.
- [13] C. Ji, S. Jie, P. Braunstein, and B. G. Li, “Fast and controlled ring-opening polymerization of  $\delta$ -valerolactone catalyzed by benzoheterocyclic urea/MTBD catalysts,” *Catal. Sci. Technol.*, vol. 10, no. 22, pp. 7555–7565, 2020, doi: 10.1039/d0cy01551b.
- [14] M. Arcana, O. Giani-Beaune, R. Schue, F. Schue, W. Amass, and A. Amass, “Ring-opening copolymerization of racemic  $\beta$ -butyrolactone with  $\epsilon$ -caprolactone and  $\delta$ -valerolactone by distannoxane derivative catalysts: Study of the enzymatic degradation in aerobic media of obtained copolymers,” *Polym. Int.*, vol. 51, no. 10, pp. 859–866, 2002, doi: 10.1002/pi.1036.
- [15] N. Kasyapi and A. K. Bhowmick, “Nanolamellar triblock of poly-d,l-lactide- $\delta$ -valerolactone-d,l-lactide with tuneable glass transition temperature and crystallinity for use as a drug-delivery vesicle,” *RSC Adv.*, vol. 4, no. 52, pp. 27439–27451, 2014, doi: 10.1039/c4ra02745k.
- [16] X. Wang, J. L. Brosmer, A. Thevenon, and P. L. Diaconescu, “Highly Active Yttrium Catalysts for the Ring-Opening Polymerization of  $\epsilon$ -Caprolactone and  $\delta$ -Valerolactone,” *Organometallics*, vol. 34, no. 19, pp. 4700–4706, 2015, doi: 10.1021/acs.organomet.5b00442.
- [17] M. Yusuf, D. Roza, Nurfajriani, H. Gunawan, and N. Dari, “Synthesis of bis( $\beta$ -diketonato)zirconium (iv) chloride as a catalyst in the ring opening polymerizations of  $\epsilon$ -caprolactone,” *Rasayan J. Chem.*, vol. 12, no. 4, pp. 2132–2140, 2019, doi: 10.31788/RJC.2019.1245463.
- [18] Y. Permana, S. Shimazu, N. Ichikuni, and T. Uematsu, “Studies on tris (  $\beta$ -diketonato ) zirconium ( IV ); syntheses , characterization and catalytic activity for ring opening of oxiranes,” *Catal. Commun.*, vol. 6, pp. 426–430, 2005, doi: 10.1016/j.catcom.2005.03.012.
- [19] C. LIU, B. LIU, Y. lin SHAO, Z. qiang LI, and C. he TANG, “Vapor pressure and thermochemical properties of ZrCl<sub>4</sub> for ZrC coating of coated fuel particles,” *Trans. Nonferrous Met. Soc. China (English Ed.)*, vol. 18, no. 3, pp. 728–732, 2008, doi: 10.1016/S1003-6326(08)60125-9.
- [20] C. Ulker, Z. Gok, and Y. Guvenilir, “Performance comparison of commercial and home-made lipases for synthesis of poly( $\delta$ -valerolactone) homopolymers,” *J. Renew. Mater.*, vol. 7, no. 4, pp. 335–343, 2019, doi: 10.32604/jrm.2019.03819.
- [21] J. Pal, S. Sanwaria, A. Choudhary, K. Thakur, B. Nandan, and R. K. Srivastava, “Thermally Initiated Trans-esterification in Poly( $\epsilon$ -caprolactone) and Its Dependence on Molecular Weight,” *J. Polym. Environ.*, vol. 22, no. 4, pp. 479–487, 2014, doi: 10.1007/s10924-014-0669-4.
- [22] J. U. Izunobi and C. L. Higginbotham, “Polymer molecular weight analysis by 1H NMR spectroscopy,” *J. Chem. Educ.*, vol. 88, no. 8, pp. 1098–1104, 2011, doi: 10.1021/ed100461v.
- [23] J. L. Sihombing *et al.*, “Characteristic and catalytic performance of Co and Co-Mo metal impregnated in sarulla natural zeolite catalyst for hydrocracking of MEFA rubber seed oil into biogasoline fraction,” *Catalysts*, vol. 10, no. 1, 2020, doi: 10.3390/catal10010121.
- [24] J. Jitonnom, R. Molloy, W. Punyodom, and W. Meelua, “The use of aluminum trialkoxide for synthesis of poly ( $\epsilon$ -caprolactone) and poly ( $\delta$ -valerolactone): A comparative study,” *Songklanakarin J. Sci. Technol.*, vol. 40, no. 4, pp. 854–859, 2018, doi: 10.14456/sjstpsu.2018.120.
- [25] H. Abe, “Thermal degradation of environmentally degradable poly(hydroxyalkanoic acid)s,” *Macromol. Biosci.*, vol. 6, no. 7, pp. 469–486, 2006, doi: 10.1002/mabi.200600070.
- [26] M. Unger, C. Vogel, and H. W. Siesler, “Molecular weight dependence of the thermal degradation of poly( $\epsilon$ -caprolactone): A thermogravimetric differential thermal fourier

- transform infrared spectroscopy study,” *Appl. Spectrosc.*, vol. 64, no. 7, pp. 805–809, 2010, doi: 10.1366/000370210791666309.
- [27] M. Yusuf, N. Dari, and E. Utama, “PM3 Semi-Empirical Method on the Ring Opening Polymerization of  $\epsilon$ -Caprolactone Using Bis (Benzoyltrifluoroacetone) Zirconium(IV) Chloride as catalyst,” in *Journal of Physics: Conf. Series*, 2020, vol. 1462, p. 012054, doi: 10.1088/1742-6596/1462/1/012054.
- [28] R. M. Yusuf M, Pulungan AN, Irmala Sari RD, Fitri Amne DP, Siregar R, “Ring-opening Polymerization Reaction Mechanism of  $\epsilon$ -Caprolactone Catalyzed by Bis(dibenzoylmethanato) zirconium(IV) Using PM3 Semi-Empirical Method.,” *J Phys Conf Ser.*, vol. 1811, pp. 1–6., 2021, doi: 10.1088/1742-6596/1811/1/012057.
- [29] I. Nifant’ev and P. Ivchenko, “Coordination ring-opening polymerization of cyclic esters: A critical overview of DFT modeling and visualization of the reaction mechanisms,” *Molecules*, vol. 24, no. 22, 2019, doi: 10.3390/molecules24224117.